

Multi-omics landscape and clinical significance of Siglec family genes: Implications for risk stratification and front line therapies in cutaneous melanoma

Kezhu Li

the first affiliated Hospital of China Medical University

Nan Xu (✉ xunancmu@126.com)

the first affiliated Hospital of China Medical University

Research Article

Keywords: melanoma, Siglec, multi-omics, SRGN, GBP4

Posted Date: April 18th, 2022

DOI: <https://doi.org/10.21203/rs.3.rs-1540844/v1>

License: © ⓘ This work is licensed under a Creative Commons Attribution 4.0 International License.

[Read Full License](#)

Abstract

Background

Melanoma is widely recognized as the most aggressive and fatal type of skin cancer; however, effective prognostic markers are lacking. The sialic acid-binding immunoglobulin-type lectin (Siglec) gene family plays an important role in the development of tumors and immune escape, but its prognostic role in melanoma remains unknown.

Method

We downloaded simple nucleotide variations, transcriptome profiling, copy number variation data of cutaneous melanoma in TCGA, and transcriptome data of GSE91061 in GEO. 14 Siglecs genes, which were extracted for comprehensive analysis. We typed samples using consistent clustering and constructed risk score using LASSO to predict patient outcomes.

Results

Siglec genes have a high mutation frequency, with up to 8% in SIGLEC7. High expression levels of Siglecs in tumor bulk suggests a better prognosis. Siglecs also show a high degree of synergistic expression. We used unsupervised clustering to create a high expression of Siglec (HES) cluster and a low expression of Siglec (LES) cluster. The HES cluster correlated with high overall survival and increased expression levels of Siglec genes. The HES cluster also showed significant immune cell infiltration and activation of immune signaling pathways. We used least absolute shrinkage and selection operator (LASSO) regression analysis to reduce the dimensionality of Siglec cluster-related genes and constructed a prognostic model composed of SRGN and GBP4, which can risk-stratify patients in both the training and test datasets.

Conclusion

We conducted a multi-omics analysis of the Siglec family genes in melanoma and found that Siglecs play an important role in the occurrence and development of melanoma. Typing constructed using Siglecs can show risk stratification and derived prognostic models can predict a patient's risk score. In summary, Siglec family genes are potential targets for melanoma treatment as well as prognostic markers that can direct individualized treatments and improve overall survival.

Background

Melanoma is the most aggressive and deadly type of skin cancer (1). Melanoma is an immunogenic tumor and is commonly associated with ultraviolet exposure and elevated tumor mutation burden (TMB).

Immune checkpoint inhibitors (ICBs) have revolutionized the management of many cancers, especially advanced melanoma. Nearly 50% of patients are treated with anti-cytotoxic T-lymphocyte associated protein 4 (CTLA4) and anti-programmed cell death protein 1 (PD-1) antibodies, leading to tumor regression and long-term long-lasting cancer control. ICB treatment is especially effective in the treatment of melanoma (2). The clinical success of ICBs in melanoma has demonstrated that reactivating the immune system can effectively inhibit tumor growth. However, even in the best-case scenario of treatment with a combination of multiple ICBs, half of the patients do not receive a lasting benefit (3). Therefore, there is a need to identify better predictive markers as well as therapeutic targets to improve overall patient survival.

Sialic acid-binding immunoglobulin-type lectins (Siglecs) are glycan-binding immune checkpoint receptors, which are expressed primarily in immune cells and play an important role in signal transduction. By identifying glycans containing sialic acid as ligands, they help the immune system distinguish between self and non-self (4). So far, 14 Siglec genes have been identified in humans, including SIGLEC1, CD22, CD33, MAG, SIGLEC5, SIGLEC6, SIGLEC7, SIGLEC8, SIGLEC9, SIGLEC10, SIGLEC11, SIGLEC14, SIGLEC15, and SIGLEC16. Siglecs have long been associated with cancer: CD22 and CD33 are specific markers for B-cell lymphoma (5, 6) and anti-CD22 and anti-CD33 antibody therapies have also been used in clinical trials of B-cell lymphoma and myeloid leukemia (7). Siglec15 is a key regulator of osteoclast differentiation. Clinical trials targeting Siglec-15 have shown encouraging therapeutic effects. Siglecs exhibit tumor-associated expression and different mechanisms of action associated with PD-L1, which implies a potential for combating disease in PD-1/PD-L1-resistant patients. However, the overall expression of Siglec family genes in melanoma tumor cells or tumor microenvironments has not been clearly studied, and it is of great significance to study Siglecs as potential prognostic markers for melanoma.

This study analyzed multi-omics data on Siglecs, including simple nucleotide variation, copy number variation, transcriptome, and clinical data, to elucidate the role of Siglec family genes in melanoma. In addition, we focused on the typing and prognosis potential of Siglecs in melanoma.

Results

Analysis of point mutations and copy number variation in Siglec family genes

We created a mutation waterfall map of Siglec family genes in the TCGA-SKCM cohort (Figure 1A). The results showed that the mutation frequency of SIGLEC7 was the highest, reaching 8%; SIGLEC1 and CD22 mutation frequencies were as high as 7%; SIGLEC6, SIGLEC10, CD33, and SIGLEC5 mutation frequencies were 6%; whereas SIGLEC15 and SIGLEC16 had no mutations, suggesting that they were highly conservative. T > A is the main point mutation found in Siglec family genes. Copy number analysis of the TCGA-SKCM cohort revealed that the increase in the copy number of SIGLEC9, SIGLEC7, CD33, SIGLEC10,

SIGLEC8, SIGLEC6, SIGLEC5, and SIGLEC14 was greater than the frequency of loss (Figure 1B-C), while the opposite was true for SIGLEC15.

Siglec family gene expression can predict overall survival

We combined the cohorts of TCGA-SKCM and GSE91061 to obtain data of 519 patients, of which clinical follow-up information was available for 507 patients. The expression matrix of the Siglec family genes was extracted and KM analysis was performed. The results showed that 12 genes had statistical significance ($P < 0.05$), and only CD22 and SIGLEC15 had no statistical significance. Also, the prognosis of the high expression group was worse than that of the low expression group. Univariate analysis of these 14 genes showed that only MAG, CD22, SIGLEC15, and SIGLEC8 were statistically insignificant; the others were statistically significant, and were all protective genes with Hazard-Ratio > 1 . Siglec family genes have highly synergistic effects at the expression level, and the positive correlation between genes is obvious.

Siglec family genes can define melanoma typing

The consensus clustering algorithm was used for clustering in the merge queue ($n = 519$). With the increase of the consensus index, the slope of the cumulative distribution curve slightly decreased, and the degree of variability of consistent CDF was the largest (Figure 3A-B). This method produces the best clustering result (Figure 3C), and the white part of the matrix heat map is clean. We used these methods to form a Siglec cluster. Using this typing to analyze the cohort with KM analysis, we found that the prognosis of patients in the A cluster was significantly higher than that of patients in the B cluster (Figure 3D). Heat map analysis showed that 14 Siglec genes were overexpressed in the A cluster and underexpressed in the B cluster (Figure 3E). We therefore defined the A cluster as the high expression of Siglec (HES) subtype and the B cluster as the low expression of Siglec (LES) subtype. Principal component analysis (PCA) clearly grouped the HES and LES subtypes, indicating the accuracy of the consistent clustering algorithm (Figure 3F). Unsupervised clustering of HES and LES by gene set variation analysis (GSVA) showed that many immune-related Kyoto encyclopedia of genes and genomes (KEGG) pathways were enriched in the HES cluster. We estimated an enrichment score of 23 immune cell gene sets in each sample by single sample gene set enrichment analysis (ssGSEA). Except for "CD56dim.natural.killer.cell" in both groups, the enrichment scores of other immune cells were significantly higher in the HES than in the LES subtype.

Gene clustering can stratify prognoses

We analyzed the differences between the HES and LES cluster groups and selected the genes with $|\logFC| > 2$ and adjusted p-value < 0.05 to obtain a group of 181 genes. We used the Metascape website for enrichment analysis of these genes. The first three enrichment terms were "regulation of cell activation",

"leukocyte activation", and "immune effector process". Univariate Cox analysis showed that of the 181 genes, 178 genes showed significantly altered levels. The expression matrices of these 178 genes were extracted for consistent clustering, and the clustering effect was the best when $K = 2$ was used (Figure 4B). The prognosis of patients in gene cluster A was significantly better than those in gene cluster B (Figure 4C). The heat maps of these 178 genes showed that these genes were generally highly expressed in gene cluster A and had strong consistency (Figure 4D). The expression levels of the Siglec family genes in gene cluster A were significantly higher than those in gene cluster B ($p < 0.001$).

Robust prediction using the LASSO model

We used LASSO regression to construct a gene prognosis model based on the results of Cox analysis of 178 genes that showed statistical significance. The merged cohort was randomly divided into two groups: training and test sets, and the training set was selected to construct the prognosis model. With the increase of the lambda value, the coefficients of some genes become 0, indicating that these genes have little contribution to the model and can be omitted (Figure 5A). We used 10X cross-validation to calculate the partial likelihood deviance of the model. The prognostic ability of the model was the best when the number of genes in the model was two. The calculation formula of the model is: Risk score = $SRGN^* (-0.1676) + GBP4^* (-0.1537)$. Using this formula, we generated a risk score for each patient. The Sankey diagram shows that the HES cluster flows to the A cluster and then flows to the low-risk group, but there is no difference in the final survival ratio (Figure 5B). The expression levels of the Siglec family genes in the low-risk group were significantly higher than those in the high-risk group, which was consistent with the previous gene family univariate Cox analysis (Figure 5C). The risk score of the HES cluster was significantly lower than that of LES cluster, and the risk score of cluster A was also significantly lower than that of cluster B (Figure 5D). KM analysis in the training set, the test set, and the merging set showed that the patients could be divided into two groups, and the overall survival rate of high-risk patients was lower than that of low-risk patients (Figure 5E). At the same time, the ROC curve of risk score was drawn for the three cohorts. In 1-/3-/5-year scenarios, the AUC values were all greater than 0.5, indicating that the model has certain prognostic ability.

Correlation analysis of risk score

We used the CIBERSORT algorithm to calculate the infiltration ratio of 22 immune cells, and analyzed the Spearman correlation with gene and risk score of the model. GBP4 was positively correlated with CD8+ T cells and macrophage M1 levels but negatively correlated with macrophage M0/2 (Figure 6A, $p < 0.001$). The risk score was negatively associated with CD8+ T cells and macrophage M1 and positively correlated with macrophage M0 (Figure 6B). We then used the ESTIMATE algorithm to calculate stromal score, immune score, and ESTIMATE score in the merge queue. The three groups with previous high-risk scores also had high scores in this analysis (Figure 6C). The TMB in the high-risk group was higher than that in

the low-risk group (Figure 6D, $p = 0.017$). Finally, two groups of mutation waterfalls were drawn, and the mutation frequency of the low-risk group was higher than that of the high-risk group (Figure 6E).

Discussion

The overall incidence of cancer is declining, but the incidence of melanoma continues to increase at a rate of approximately 3% per year, causing severe public health problems and economic burdens (8). ICB therapy and targeted therapy for melanoma shows a good remission rate; however, good prognostic markers are lacking. In this study, we comprehensively analyzed the role of Siglec family genes in melanoma using multiple datasets and found that SIGLEC7 has a mutation frequency as high as 8%. Siglec genes are protective factors of melanoma. Consistent clustering can divide melanoma patients into a Siglecs high-expression group and a Siglecs low-expression group, with the high-expression group indicating a better prognosis. In short, Siglecs are a potential therapeutic target and prognostic marker for melanoma.

The Siglec family genes play an important role in the occurrence and development of melanoma. The mutation frequency of SIGLEC7 is up to 8% in melanoma, whereas those of SIGLEC1 and CD22 are up to 7%. Siglec family genes play an important role in tumor formation and may be some of the key genes that drive normal cells to evolve into tumor cells. Siglec family genes are thought to mainly act in immune cells (4), but little is known about the mechanism of action in tumor cells. Copy number variation in SIGLEC15 melanoma is mainly loss, whereas other Siglec family genes are mainly acquired. SIGLEC15 is expressed in tumor cells, and anti-SIGLEC15 mAb inhibitors can significantly upregulate the immunosuppressive function of colorectal cancer in mice (9). Although there are structural and functional similarities between SIGLEC15 and PD-L1, the immunosuppressive mechanism mediated by SIGLEC15 seems to be independent of the PD pathway; therefore, SIGLEC15 is the most promising alternative candidate for drug-resistant PD-L1 patients.

Siglec family genes are highly coexpressed, and the high expression of most genes indicates a higher survival rate. Some studies inhibit tumor growth through intravenous injections of abiotic sialic acid on the surface of melanoma tumor cells to guide the recognition and binding of SIGLEC1 by macrophages (10). Studies also showed that macrophages expressing SIGLEC1 in the subcapsular sinus provide the correct environment for melanoma lymph node metastasis (11). However, other studies have shown that SIGLEC1 can inhibit tumor growth, and SIGLEC1-positive macrophages inhibit melanoma by limiting tumor-derived vesicle-B cell interaction (12). SIGLEC1-positive macrophages are closely related to T cell-mediated anti-tumor immunity (13). The degree of infiltration of CD33-positive bone marrow cells may indicate a poor prognosis of patients with melanoma (14). Most of the tumor-infiltrating CD8 + T cells in melanoma specimens express SIGLEC9, which binds to the ligands on the surface of tumor cells, thus inhibiting T-cell response in the tumor microenvironment (15). These studies focus on the expression of the Siglec gene in a single immune cell, and the results show that Siglecs can help tumors achieve immune escape.

The expression levels of Siglecs in this study represent the overall level expressed in the tumor microenvironment, and Siglecs are expressed in a variety of immune cells. Our analysis shows that high expression levels of Siglecs suggest immune cell infiltration and activation of immune-related signaling pathways. Infiltrating immune cells can lead to a better prognosis for patients with melanoma (16). This finding explains why the high expression levels of Siglecs in the transcriptional group of melanoma bulk is associated with a better prognosis for patients.

Siglec cluster classification is a prognostic marker of melanoma. We used consistent clustering to obtain HES and LES clusters from the Siglec family gene expression data. The HES cluster is characterized by consistent and high expression levels of Siglecs, which suggests a better clinical prognosis, whereas the LES cluster is the opposite. Twenty-one types of immune cells (mainly B cells, CD4 + T cells, and CD8 + T cells) in the HES cluster showed a high level of infiltration. GSVA showed that the immune activation-related signal pathway of the HES cluster was abnormally activated, whereas the opposite was true for the LES cluster. Fourteen Siglec genes were overexpressed in the A cluster and underexpressed in the B cluster, and these genes showed very strong co-expression, strengthening the clustering results.

To further explore the differences between groups contained in the Siglec cluster, we analyzed the differences in the expression profiles of A and B clusters. We enriched and analyzed the identified genes, and the results showed that these genes were mainly involved in the activation of immune cells, including innate and adaptive immune cells. Tumor samples can still be grouped by using these genes for unsupervised clustering again, and both Siglecs and differentially expressed genes were consistently highly expressed in the A cluster. These differentially expressed genes may have a very close interaction with Siglecs. Moreover, we used these genes for LASSO regression analysis to construct the risk scores of SRGN and GBP4. The risk scores were successfully verified by both the training set and the test set. The predictive performance of this model is similar to that of the Siglec cluster, but it has a stronger clinical application prospect because of the small number of genes. GBP4 was positively correlated with CD8 + T cells and macrophage M1 levels but negatively correlated with macrophage M0/2 levels. GBP4 is a guanosine monophosphate binding protein, and many studies have shown that GBP4 is a good prognostic marker for melanoma (17, 18). The detection of these markers in tumor tissues and patients' sera revealed that melanoma has an obvious heterogeneity due to which the markers found are not universally applicable (19). The Siglec cluster developed in this study and the gene cluster and risk score based on the Siglec cluster have a very strong prognostic effect and have potential clinical application value.

Although this study uses multi-omics to analyze the role of the Siglec family genes in melanoma, there are still some shortcomings. First, this study is based on the bulk data of tumor tissue, without specific analysis of Siglecs in immune cells; second, the typing and model constructed need an expanded clinical cohort for verification; third, although our findings show that Siglecs play an important role in the occurrence and development of melanoma, further experiments are needed to elucidate the mechanism.

Conclusion

We systematically analyzed multiple sets of data pertaining to Siglec gene family expression in melanoma. We found that Siglecs have a high mutation frequency and that a higher expression levels of Siglecs indicated better prognosis among patients. We believe the mechanism of action of Siglecs may involve immune cell infiltration and immune signal pathway activation. Our work points to Siglecs as both important prognostic markers for creating individualized treatment plans for patients, as well as drug targets to treat this aggressive and fatal disease.

Methods

Data acquisition

We downloaded data pertaining to the skin cutaneous melanoma (SKCM) multi-group cohort from The Cancer Genome Atlas (TCGA, <https://portal.gdc.cancer.gov/>), including 472 simple nucleotide variations in VarScan2 annotation format, 472 transcriptome profiles in HTSeq-FPKM format, and 470 clinical data. The downloaded raw data were sorted using Perl (<https://www.perl.org/>). From the UXSC Xena website (<https://xena.ucsc.edu/>) (20), we downloaded 367 sets of copy number variation data in GISTIC2 format. We downloaded transcriptome data from GSE91061 (FPKM format) from the Gene Expression Omnibus (GEO, <https://www.ncbi.nlm.nih.gov/gds>), specifically the melanoma immunotherapy cohort (21). We converted the TCGA-SKCM and GSE91061 transcript group data to TPM format using the R package "limma". We used the R packages "limma" and "sva" to merge TCGA-SKCM and GSE91061 into one cohort (n = 519). The above data analysis and the following analysis were performed using R software (R x64 4.1.0).

Simple nucleotide variation and copy number variation data analysis

Using the R package "maftools", 14 Siglec family genes were extracted to draw the waterfall map. We used Perl to calculate the TMB value, which here refers to the relative number of gene mutations in a particular tumor tissue, and its calculation principle is Fisher's exact test of VarScan2. The copy number variation data were also sorted out into a gene matrix using Perl. We used the R package "RCircos" to draw a circle map of the position of the gene on the chromosome.

Consensus clustering and principal component analysis

Consensus clustering is an unsupervised clustering method that can classify subtypes of samples according to genetic multiplex data. The basic principle of the algorithm is to use the resampling method to extract a certain sample data set and calculate the rationality of the specified number of clusters. A consistent cumulative distribution function (CDF) diagram and Delta area plot of CDF can be drawn according to different K values (K values from 1 to 9). When the initial speed of CDF is slow, the best K

value is selected according to the cleanliness of the clustering result background and the actual clinical situation. The algorithm is based on the R package "ConsensusClusterPlus". PCA was used to identify the results of consensus clustering, based on the R packages "limma" and "ggplot2".

Least absolute shrinkage and selection operator

LASSO is an algorithm that filters variables through data dimensionality reduction. By constructing a penalty function, it can compress the coefficients of variables and change some regression coefficients to 0, to achieve the purpose of variable selection. In this study, the merging cohort was randomly divided into a training dataset and a test dataset with a proportion of 1:1. We used the LASSO algorithm to construct a robust and simple prognostic model in the training dataset. The model formula can be used to calculate the risk score of each patient. The prediction performance of the model can be judged by using the training dataset and the test dataset for Kaplan-Meier (KM) analysis. The above calculation flow is based on the R package "glmnet" (22).

Enrichment analysis

ssGSEA is an extension of the gene set enrichment analysis (GSEA) method, which calculates the enrichment fraction (23) of each sample and gene set pair. ssGSEA can calculate the final enrichment score of a single sample based on the gene set, thus judging the pathway or the activity of specific cells. We downloaded the gene sets of immune cells from the ImmPort website (<https://www.immport.org/home>). Through analysis of the immune cell gene set, the ssGSEA algorithm can be used to evaluate the activity of immune cells in each sample. GSVA, an algorithm of GSEA (24), can classify samples unsupervised with respect to the changes of pathway activity according to the amount of gene expression and multiple pathway information. As a result of this analysis, we obtained pathways with differences in different groups. Metascape (<http://metascape.org>) integrates more than 40 bioinformatics databases (25), including those related to biological pathway enrichment analysis, protein-protein interaction network structure analysis, and rich gene annotation functions.

CIBERSORT and ESTIMATE algorithm

CIBERSORT is a deconvolution tool for the expression matrix of human immune cell subtypes based on the principle of linear support vector regression (26). LM22 in CIBERSORT's report is a signature gene expression matrix used to estimate the proportion of white blood cells in bulk RNA, where LM22 and bulk RNA are linked by machine learning. When the bulk RNA data are entered into this program, the proportion of immune cell infiltration can be calculated. ESTIMATE is an algorithm for evaluating the purity of tumor samples (27). Stromal score and immune score can be calculated by estimating the expression matrix of tumor samples, which can be used to represent the existence of matrix and immune cells. The estimate

score, which can be used to estimate the purity of the tumor, can be obtained by adding the stromal and immune score.

Survival analysis

KM analysis, the most widely used method of survival analysis at present, is a non-parametric method to estimate the survival probability from the observed survival time. We used the R packet "survminer" and "survival" to find the threshold of the best grouping of 14 genes, and then divided them into two groups for KM analysis. The receiver operating characteristic (ROC) curve is also known as the sensitivity curve; the grouping of points on the curve reflects that they all respond to the same signal stimulus. The area under curve (AUC) is defined as the area surrounded by the coordinate axis under the ROC curve. When the AUC is greater than 0.5, the classifier has a certain role. We used the ROC curve to judge the prognostic ability of the model.

Other analysis and statistical analysis

All of heat map in this study was prepared using the "pheatmap" R package; the column scatter chart and violin chart were prepared using "ggpubr" and "reshape2"; and the Sankey diagram was generated using "ggalluvial". The comparison between the two groups was performed using the difference analysis algorithm "limma", and the correlation analysis was performed using the Spearman test.

Declarations

Ethics approval and consent to participate

Not applicable

Consent for publication

Not applicable

Availability of data and materials

You can obtain the TCGA-SKCM cohort from The Cancer Genome Atlas database. And obtain GSE91061 cohorts from the Gene Expression Omnibus.

Competing interests

The authors declare that they have no competing interests

Funding

Not applicable

Authors' contributions

Kezhu Li conducted data analysis and written manuscripts, Nan Xu provided ideas and designed experiments.

Acknowledgements

We are grateful for the free use of TCGA and GEO databases.

References

1. Huang A, Zappasodi R. A decade of checkpoint blockade immunotherapy in melanoma: understanding the molecular basis for immune sensitivity and resistance. *Nature immunology*. 2022.
2. Carlino M, Larkin J, Long G. Immune checkpoint inhibitors in melanoma. *Lancet (London, England)*. 2021;398(10304):1002-14.
3. Wolchok J, Chiarion-Sileni V, Gonzalez R, Grob J, Rutkowski P, Lao C, et al. Long-Term Outcomes With Nivolumab Plus Ipilimumab or Nivolumab Alone Versus Ipilimumab in Patients With Advanced Melanoma. *Journal of clinical oncology : official journal of the American Society of Clinical Oncology*. 2022;40(2):127-37.
4. Duan S, Paulson J. Siglecs as Immune Cell Checkpoints in Disease. *Annual review of immunology*. 2020;38:365-95.
5. Ricart A. Antibody-drug conjugates of calicheamicin derivative: gemtuzumab ozogamicin and inotuzumab ozogamicin. *Clinical cancer research : an official journal of the American Association for Cancer Research*. 2011;17(20):6417-27.
6. Sullivan-Chang L, O'Donnell R, Tuscano J. Targeting CD22 in B-cell malignancies: current status and clinical outlook. *BioDrugs : clinical immunotherapeutics, biopharmaceuticals and gene therapy*. 2013;27(4):293-304.
7. Mims A, Stuart R. Developmental therapeutics in acute myelogenous leukemia: are there any new effective cytotoxic chemotherapeutic agents out there? *Current hematologic malignancy reports*. 2013;8(2):156-62.
8. Tripp M, Watson M, Balk S, Swetter S, Gershenwald J. State of the science on prevention and screening to reduce melanoma incidence and mortality: The time is now. *CA: a cancer journal for clinicians*. 2016;66(6):460-80.
9. De Henau O, Rausch M, Winkler D, Campesato L, Liu C, Cymerman D, et al. Overcoming resistance to checkpoint blockade therapy by targeting PI3K γ in myeloid cells. *Nature*. 2016;539(7629):443-7.
10. Xie Y, Li Y, Han S. Metabolic installation of macrophage-recruiting glycan ligand on tumor cell surface for in vivo tumor suppression. *Bioorganic & medicinal chemistry letters*. 2022;57:128500.
11. Singh R, Choi B. Siglec1-expressing subcapsular sinus macrophages provide soil for melanoma lymph node metastasis. *eLife*. 2019;8.

12. Pucci F, Garris C, Lai C, Newton A, Pfirschke C, Engblom C, et al. SCS macrophages suppress melanoma by restricting tumor-derived vesicle-B cell interactions. *Science (New York, NY)*. 2016;352(6282):242-6.
13. Saito Y, Ohnishi K, Miyashita A, Nakahara S, Fujiwara Y, Horlad H, et al. Prognostic Significance of CD169+ Lymph Node Sinus Macrophages in Patients with Malignant Melanoma. *Cancer immunology research*. 2015;3(12):1356-63.
14. Choi J, Kim Y, Yun K, Won C, Lee M, Choi J, et al. The prognostic significance of VISTA and CD33-positive myeloid cells in cutaneous melanoma and their relationship with PD-1 expression. *Scientific reports*. 2020;10(1):14372.
15. Haas Q, Boligan K, Jandus C, Schneider C, Simillion C, Stanczak M, et al. Siglec-9 Regulates an Effector Memory CD8 T-cell Subset That Congregates in the Melanoma Tumor Microenvironment. *Cancer immunology research*. 2019;7(5):707-18.
16. Fridman W, Pagès F, Sautès-Fridman C, Galon J. The immune contexture in human tumours: impact on clinical outcome. *Nature reviews Cancer*. 2012;12(4):298-306.
17. Qu Y, Zhang S, Zhang Y, Feng X, Wang F. Identification of immune-related genes with prognostic significance in the microenvironment of cutaneous melanoma. *Virchows Archiv : an international journal of pathology*. 2021;478(5):943-59.
18. Wang Q, Wang X, Liang Q, Wang S, Xiwen L, Pan F, et al. Distinct prognostic value of mRNA expression of guanylate-binding protein genes in skin cutaneous melanoma. *Oncology letters*. 2018;15(5):7914-22.
19. Donnelly D, Aung P, Jour G. The "-OMICS" facet of melanoma: Heterogeneity of genomic, proteomic and metabolomic biomarkers. *Seminars in cancer biology*. 2019;59:165-74.
20. Goldman M, Craft B, Hastie M, Repečka K, McDade F, Kamath A, et al. Visualizing and interpreting cancer genomics data via the Xena platform. *Nature biotechnology*. 2020;38(6):675-8.
21. Riaz N, Havel J, Makarov V, Desrichard A, Urba W, Sims J, et al. Tumor and Microenvironment Evolution during Immunotherapy with Nivolumab. *Cell*. 2017;171(4):934-49.e16.
22. Friedman J, Hastie T, Tibshirani R. Regularization Paths for Generalized Linear Models via Coordinate Descent. *Journal of statistical software*. 2010;33(1):1-22.
23. Barbie D, Tamayo P, Boehm J, Kim S, Moody S, Dunn I, et al. Systematic RNA interference reveals that oncogenic KRAS-driven cancers require TBK1. *Nature*. 2009;462(7269):108-12.
24. Hänzelmann S, Castelo R, Guinney J. GSVA: gene set variation analysis for microarray and RNA-seq data. *BMC bioinformatics*. 2013;14:7.
25. Zhou Y, Zhou B, Pache L, Chang M, Khodabakhshi A, Tanaseichuk O, et al. Metascape provides a biologist-oriented resource for the analysis of systems-level datasets. *Nature communications*. 2019;10(1):1523.
26. Newman A, Liu C, Green M, Gentles A, Feng W, Xu Y, et al. Robust enumeration of cell subsets from tissue expression profiles. *Nature methods*. 2015;12(5):453-7.

27. Yoshihara K, Shahmoradgoli M, Martínez E, Vegesna R, Kim H, Torres-Garcia W, et al. Inferring tumour purity and stromal and immune cell admixture from expression data. *Nature communications*. 2013;4:2612.

Figures

Figure 1

Analysis of mutation and copy number variation (CNV) of Siglec family genes. (A) Mutation waterfall. (B) The frequency of CNVs. (C) A circle map of the position of the gene on the chromosome. Red indicates an increase in CNVs, and blue indicates a decrease in CNVs.

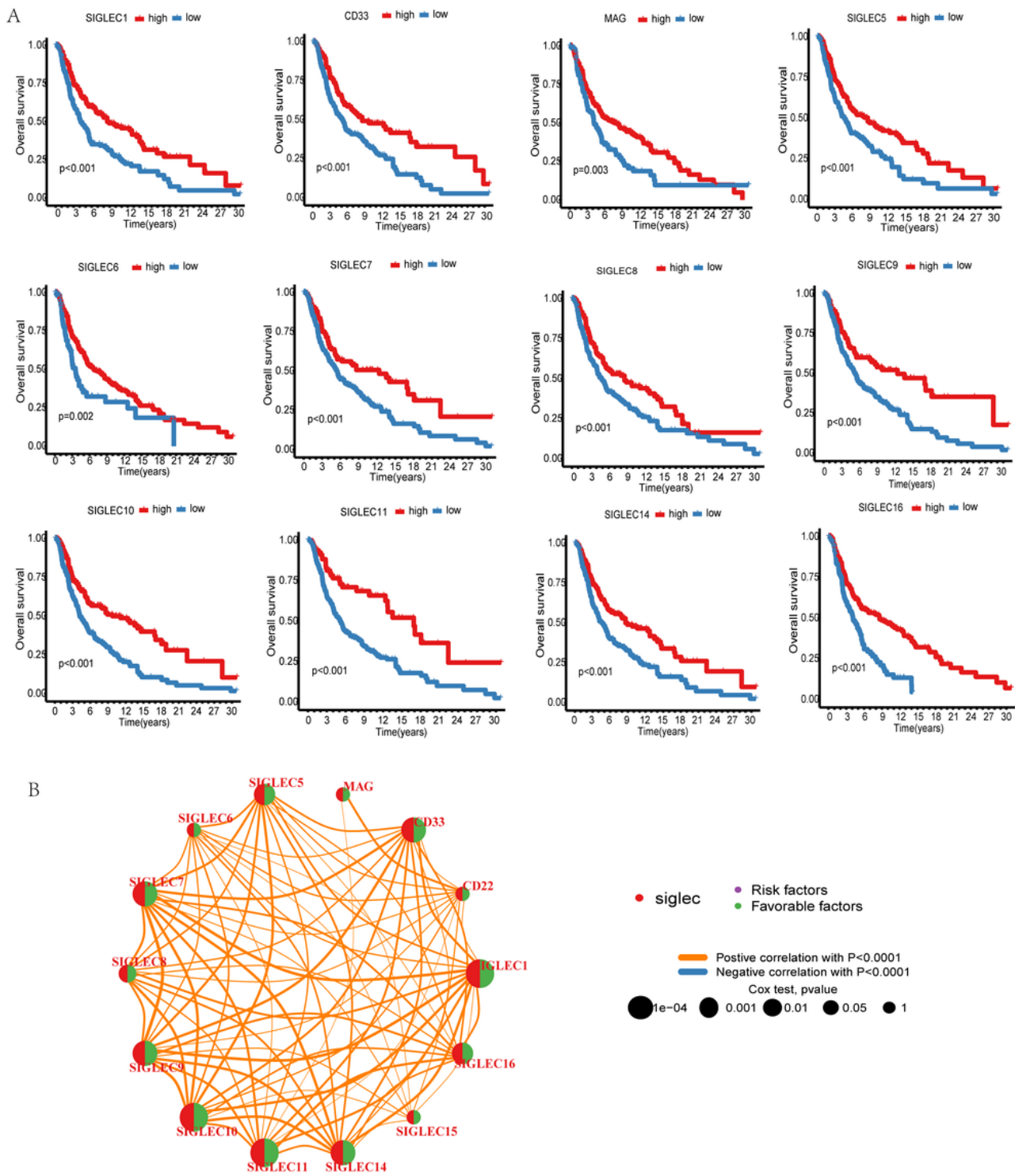


Figure 2

Survival analysis of Siglec family genes. (A) Kaplan-Meier analysis of 12 genes. (B) The results of Cox analysis of Siglec family genes and gene coexpression network.

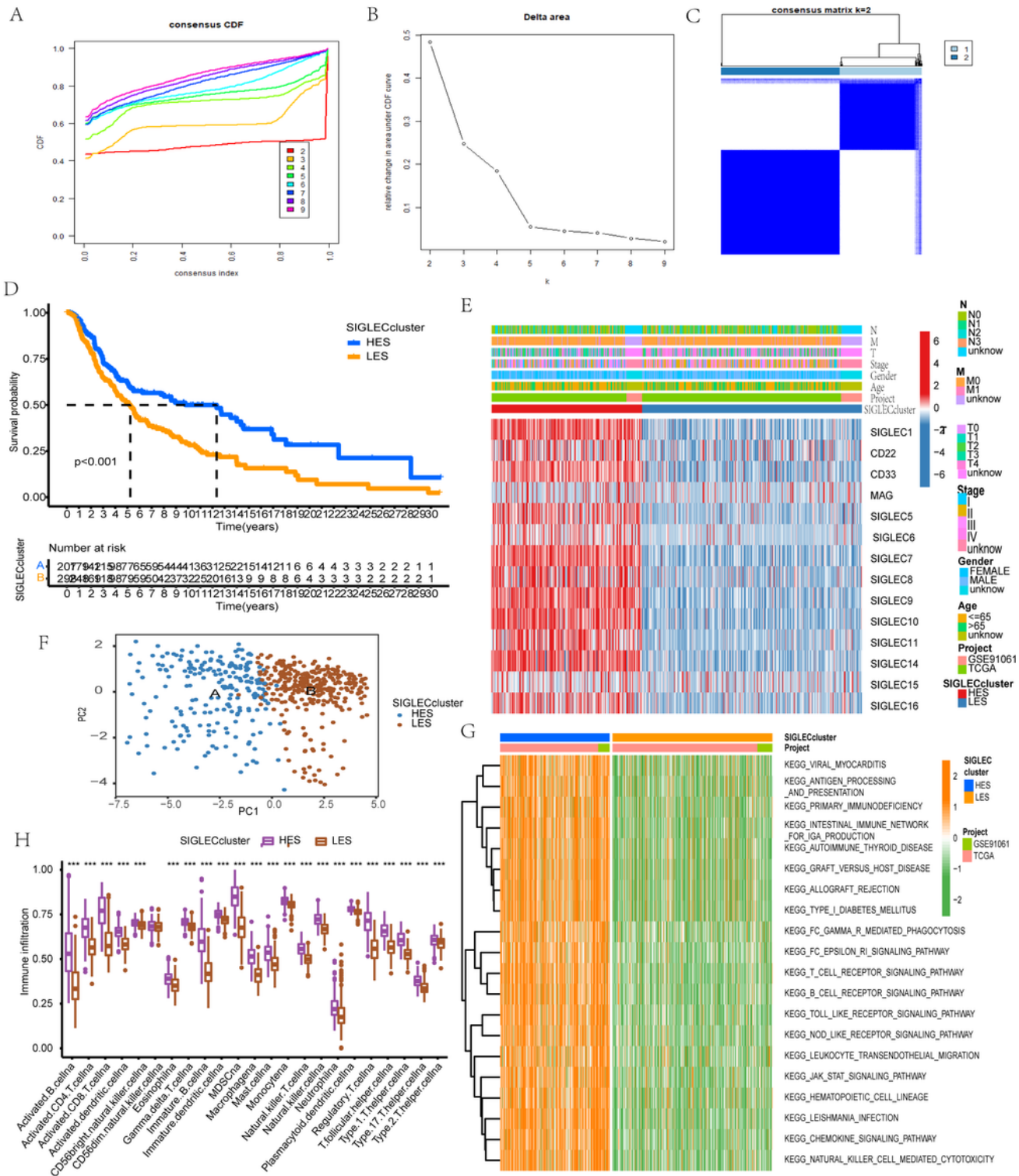


Figure 3

Siglec family genes can define melanoma typing. (A) The cumulative distribution curve corresponding to different K values. (B) The relative change in the area under the curve of the cumulative distribution function (CDF). (C) The sample-consistent cluster diagram when K = 2. (D) Kaplan-Meier (KM) analysis was carried out according to the Siglec cluster. (E) The expression heat map of Siglec family genes and the clinical information distribution of the cohort. (F) Principal component analysis (PCA) of the Siglec

cluster. (G) Enrichment result of the gene set variation analysis (GSVA) pathway. (F) The single sample gene set enrichment analysis (ssGSEA) and evaluation scatter plot of immune cells.

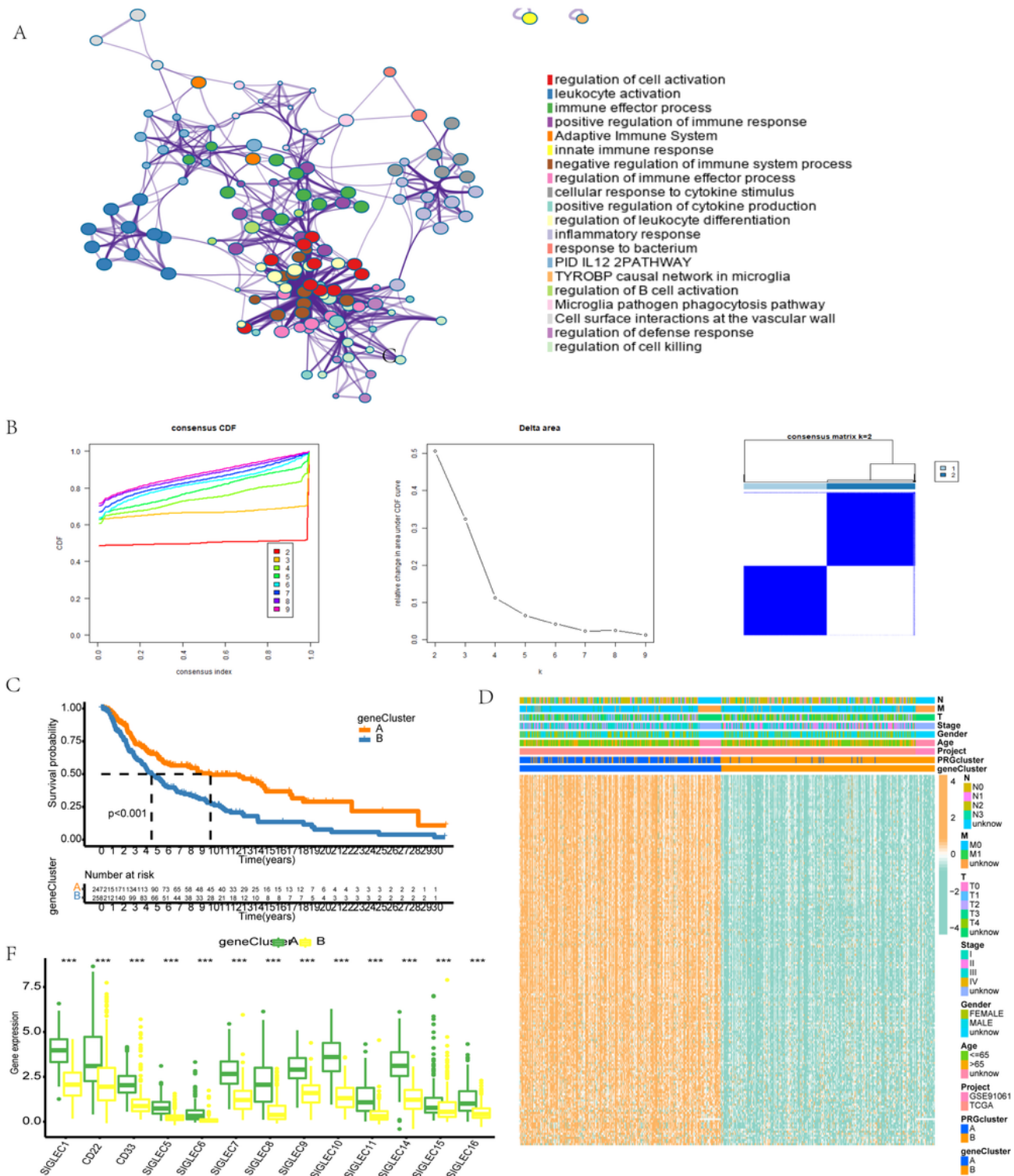


Figure 4

Correlation analysis of differentially expressed genes in the Siglec cluster. (A) The results of enrichment analysis using Metascape. (B) Consistent cluster analysis. The graph on the left shows the cumulative

distribution curve, the middle graph shows the area change under the cumulative distribution curve, and the figure on the right shows the clustering results of the samples at $K = 2$. (C) The results of gene clustering analysis. (D) Heat map of gene expression related to genotyping. (F) Differential expression of Siglec family genes in gene cluster A and gene cluster B. "***", "**" and "*" mean "0.001", "0.01" and "0.05", respectively.

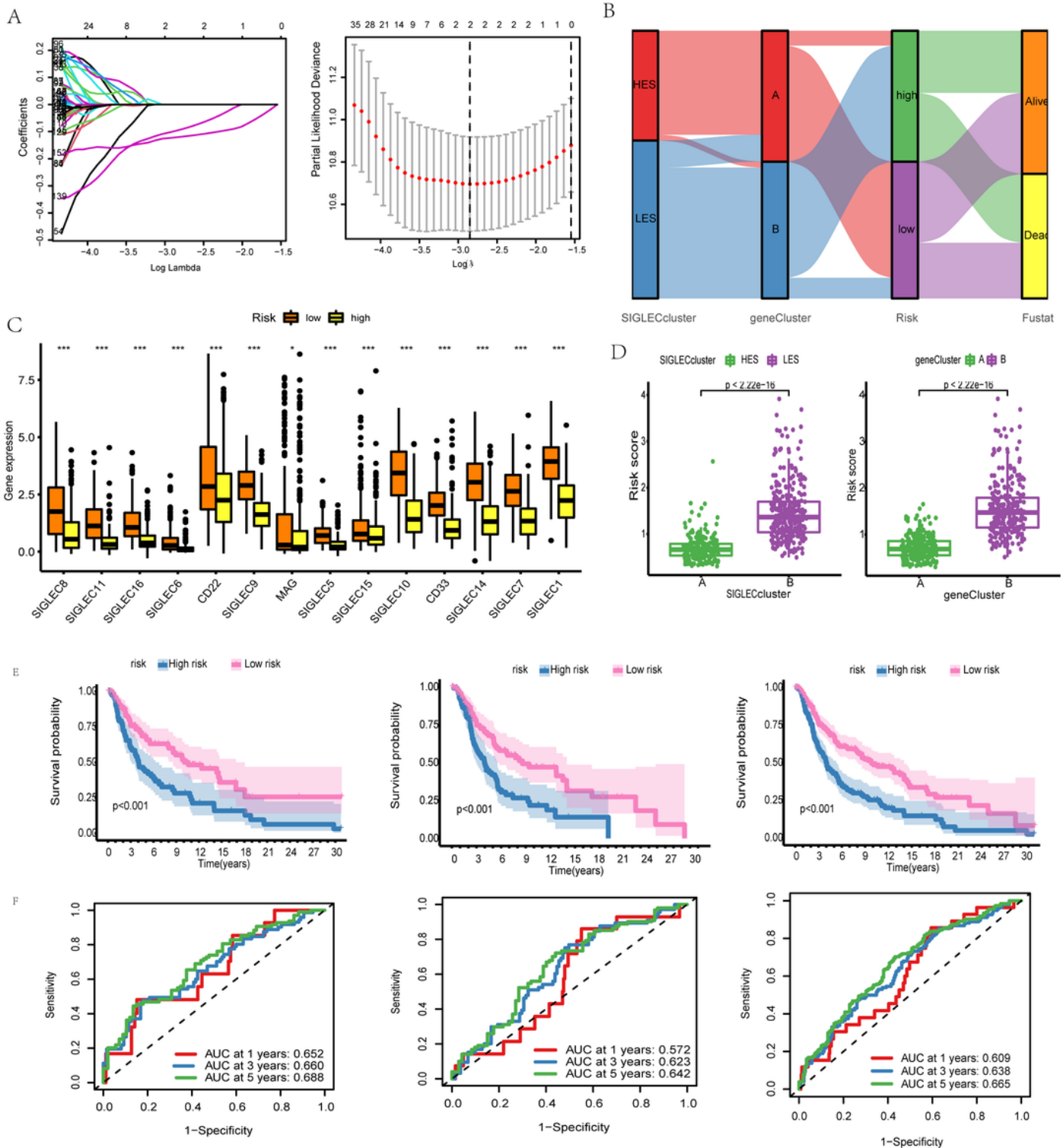


Figure 5

The genetic model can provide robust prediction. (A) On the left is the lambda and gene coefficient curve, and on the right is the result of 10x cross validation. (B) Sankey diagram for the Siglec cluster, the gene cluster, risk, and fustat. (C) Fourteen genes were expressed differently in the high-risk group and the low-risk group. (D) The scatter plot of risk score difference between the Siglec cluster and the gene cluster. (E) Kaplan-Meier (KM) analysis was performed in the training set, the test set, and the all set. (F) Receiver operating characteristic (ROC) curves of the training set, the test set, and the all set.

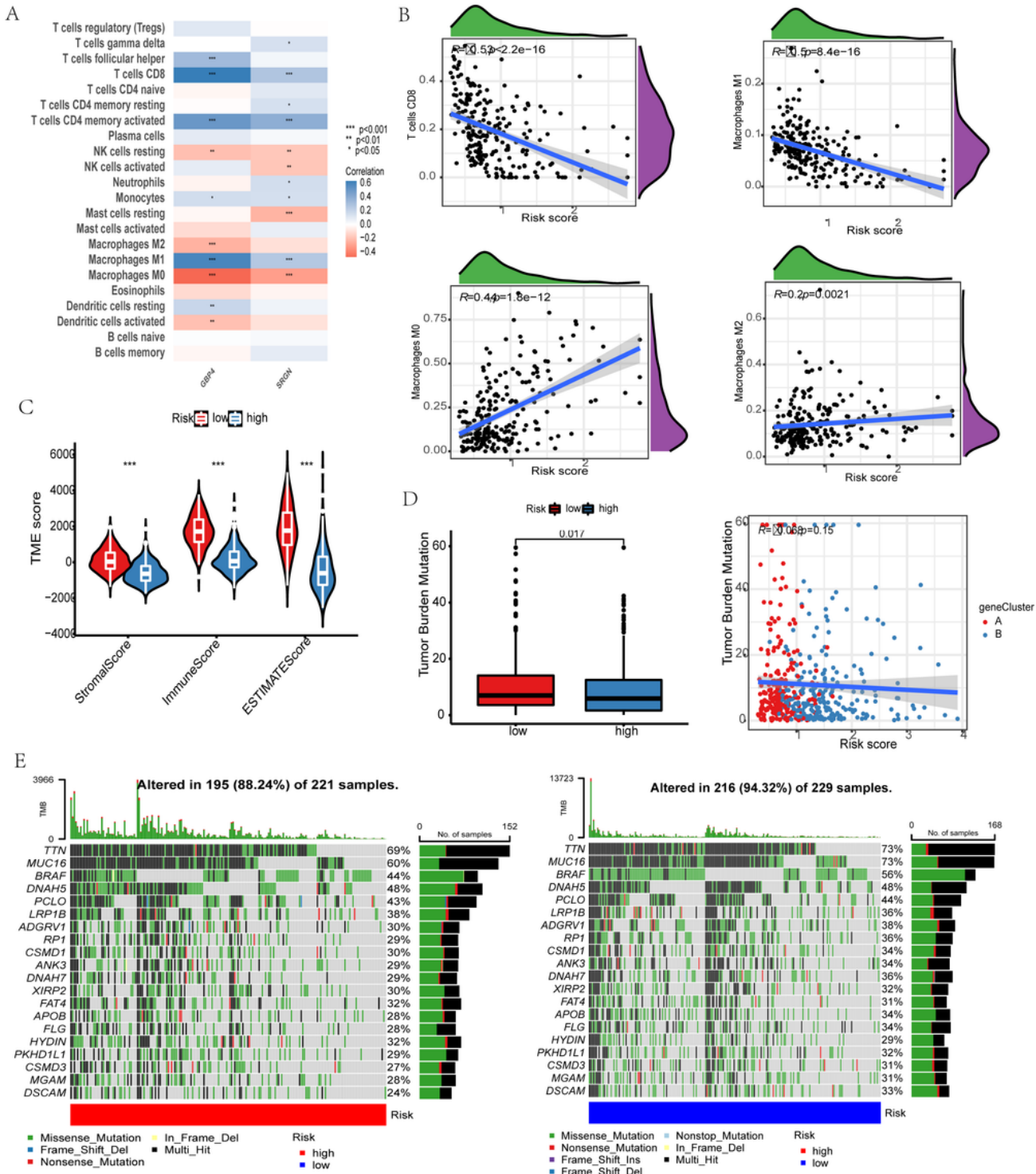


Figure 6

Risk score correlation analysis. (A) Correlation analysis between GBP4, SRGN, and the level of immune cell infiltration. (B) The scatter plot of the correlation between the risk score and CD8+ T cells, macrophage M1 memory macrophage M0, and macrophage M2. (C) Violin chart of ESTIMATE score difference between high- and low-risk groups. (D) The left image shows the tumor mutation burden (TMB) difference analysis of the high- and low-risk groups, and the right image shows the scatter plot of TMB and risk score. The red dot is cluster A and the blue dot is cluster B. (E) The image on the left shows the point mutation waterfall of the high-risk group, and the image on the right shows the point mutation waterfall of the low-risk group.